Controlling Liquid Release by Compressing Electrospun Nanowebs

K.G. Kornev[1], X. Ren[2], Y. Dzenis[2]

[1]Clemson University, Clemson, South Carolina UNITED STATES

[2]University of Nebraska, Lincoln, Nebraska UNITED STATES

Correspondence to:
Kostantin G. Kornev email: kkornev@clemson.edu

ABSTRACT

Electrospun nanowebs with pores ranging from nanometers to micrometers, constitute new materials with enhanced absorbency and ability to retain liquids in pores for a long period of time. These materials can be used as nanofluidic probes collecting minute amount of liquids. However, extraction of liquids from nanofibrous materials presents a problem: menisci in the interfiber pores create very high suction pressure which holds the liquid inside the material. This problem can be resolved if the probe is completely filled with the liquid: menisci at the probe edges become flat to establish a pressure equilibrium with the atmosphere. Therefore, one can take advantage of the nanoweb softness and extract liquid by mechanically deforming the nanowebs. We show that the liquid-saturated nanowebs follow the Voigt-type rheology upon loading. We theoretically explain this behavior and derive the relations between the Voigt phenomenological parameters, nanoweb permeability and compression modulus. We show that the limiting deformations follow the Hooke's law which assumes linear relation between the extracted volume of liquid and the applied load. Because of this predictable behavior, the nanoweb probes can be engineered to release minute liquid doses upon compression. The developed experimental methodology can be used for characterization of nanostructured materials which otherwise impossible to analyze by using the existing instruments.

INTRODUCTION

Probing and analysis of biofluids from secretory glands, ducts, and microorganisms call for development of specific micro and nanofluidic devices. If one has to probe the liquid from microducts, the pore in the probing tip must be less than the duct size. This guaranties that the liquid will be sucked into probe by capillary action. To analyze the liquid, one has to push the droplet out from the probing tip. The applied pressure needed to displace the liquid from the pores must be comparable with the capillary pressure. For water in the hundred nanometer pore the suction pressure is about hundred meters of water column! Hence, there is a dilemma: introducing nanofeatures to build high suction pressure in the probing material, one has to apply a comparable pressure to push the liquid out of the pores for further chemical analysis. Therefore, the hydraulic pumps must provide sufficiently high pressure to displace the liquid from the probing tip. However, the hydraulic pumps are undesirable features in the micro and nanofluidic devices.

The problem can be resolved if the material becomes completely saturated with the liquid, so that the menisci in the pores are flattened. In this case, the pressure difference between the liquid in the probe and the atmosphere disappears. As probing materials, we suggest to use compliant electrospun nanowebs [2-5]. Upon compression, these materials, like sponges, squeeze the liquid out of pores. In this design, there is no need for hydraulic pumps: due to capillary action the liquid is sucked into the nanoweb spontaneously. After complete probe saturation, the liquid extraction is obtained by mechanical squeezing the material.

As probing materials, electrospun nanowebs have some advantages: they contain mesopores at nanofiber crossings and transport pores of micrometer radii formed by the nanofiber assembly (*Fig.1*). The mesopores provide high suction

pressure, while transport pores assure fast absorption. The process of absorption by materials with a hierarchical pore structure has been discussed in recent publications [6-8].

In this paper, we discuss the mechanism of liquid release when the nanoweb is subjected to compression.

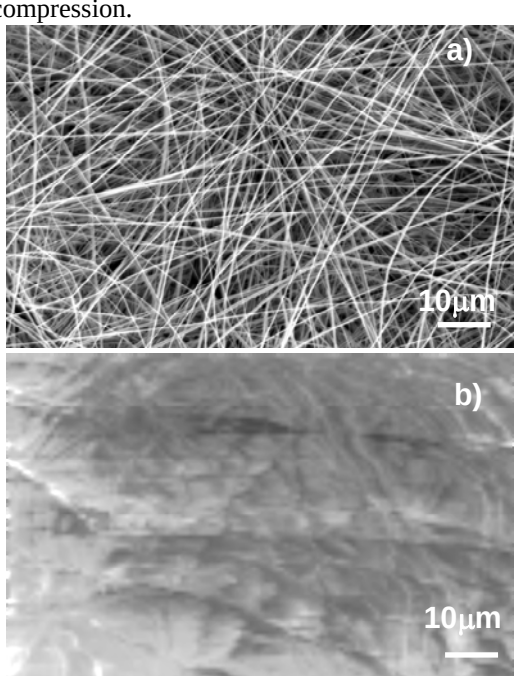

FIGURE 1. Electrospun nanoweb from vinylidene fluoride and trifluoroethylene a) dry and b) filled with silicone oil.

There are several experimental and theoretical approaches aimed at quantitative analysis of the deformation effects in porous materials filled with liquids [9-12] . Experimental works mostly deal with the forced injection of liquids in deformable porous materials [13,14]. Here we describe new approach, which allows us to assess some mechanical characteristics of thin porous samples. We consider our method as a complementary to the beam-bending method proposed by G. Scherer [15,16]. The proposed method shows a practical way to characterize nanofibrous webs and to estimate the materials capability for dosing liquids given in minute amounts.

MATERIALS

Nanowebs used in this work were produced by electrospinning method. Electrospinning is an emerging nanomanufacturing technology capable of producing continuous nanofibers down to several nanometers in diameter [2-4,17]. In this inexpensive method, nanofibers are spun from polymer solutions at high electric fields. A jet is ejected from a nozzle or a free surface at a certain threshold voltage. These charged jets are stretched on their way to collector and gathered in the form of continuous nanofiber web. The morphology of nanofibers and nanowebs are controlled by the type of the solvent, solution properties, electric field configuration and some other process parameters [2,3,17-19]. Nanowebs used in this work (*Fig.1*) were produced from copolymer viny-lidene flouride and trifluoroethylene, P(VDF-TrFE) with 65% molar content of vinylidene fluoride. We used 24% w/w P(VDF-TrFE) in dimethylformamide (DMF). The flow rate was 0.15ml/h. The tip to collector distance was 25cm and the applied voltage was 14kV. The voltage was first generated by a DC power supply (Hewlett - Packard E3611A) then amplified by a DC amplifier (Gamma High Voltage Research UC5 - 20P). The details of the process can be found in Ref. [20]

SQUEEZING DEFORMATIONS OF NANOWEBS

Experimental setup is shown schematically in *Fig.2*. A nanoweb saturated with the liquid is sandwiched between two impermeable plates. The liquid is supposed to wet these plates. The sample is compressed by an external load. Due to compression, the sample squeezes the liquid out. Assume that the known load does not change in time. Therefore, the dynamics of the sample thinning is completely controlled by the elastic and hydraulic reaction of the sample. To describe the flow, we introduce the following assumptions: a) the fibers constituting the sample skeleton are considered incompressible; b) because of an enhanced friction between fibers, thin nonwoven materials are difficult to deform in plane by compressing them transversely [21,22]. Therefore, we assume that the in-plane deformations are insignificantly smaller than the trans-plane deformations, i.e. the sample does not change its area during deformations. Thus, the total deformation consists of localized fiber bending at the fiber crossings (with zero volumetric strain at the fiber scale) and by possible reversible sliding of one fiber over another. These two deformation mechanisms lead to an elastic reaction of the sample skeleton. We do not consider irreversible sliding of fibers in this model.

Using these assumptions, we can show (the details are given in the Appendix) that the sample behavior is similar to the behavior of a viscoelastic material described by the Voigt-type rheology model (see *Fig.2b* for mechanical interpretation of the model). The spring in *Fig 2b*) models an elastic response of

the fibrous skeleton, and the dashpot models the hydraulic resistance of the draining fluid. As shown in the Appendix, at the initial moments of time, when the spring and dashpot are both forced to move at constant rate, the friction force exerted by the dashpot

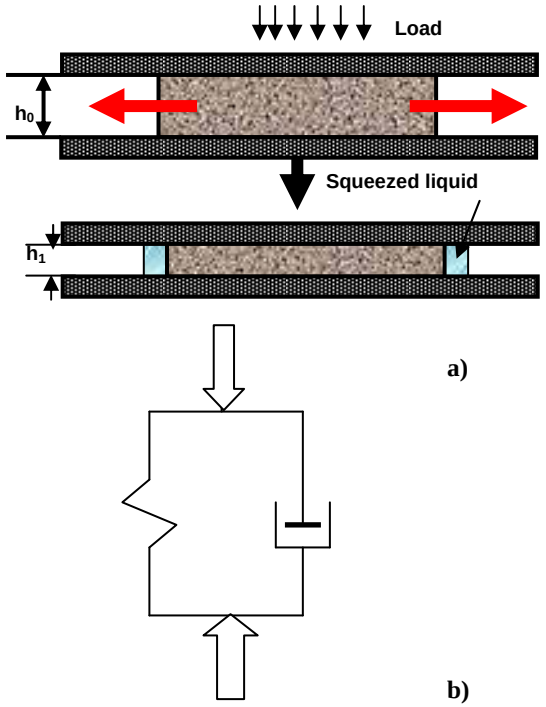

FIGURE 2 a). External load (vertical arrows) compresses the porous sample sandwiched between impermeable plates. The sample deforms and changes its thickness from h_0 to h_1. The liquid saturating the sample flows out of the sample (horizontal arrows). b) The Voigt dashpot-spring model [1] of a saturated porous sample.

stabilizes the elastic reaction of the spring and the total force remains constant. When the force is applied to the Voigt element, one observes an exponential relaxation of the sample thickness toward a new equilibrium value (see the discussion in the Appendix).

Assuming also that the sample is a circular disk of radius R and thickness h, $h << R$, the parameters of the Voigt model can be connected to the physical parameters of the fibrous material and the liquid. We describe an isotropic fibrous material as a Hooke's elastic body and assume that the flow follows the Darcy's law. Thus, the relation between the pressure gradient and velocity of liquid particles is linear, $\mathbf{v} = -(k/\eta)\nabla p$,where η is viscosity and k is the sample permeability, which is a function of the sample deformations [10]. If the deformations are small, the model predicts an exponential relaxation of the sample toward a new equilibrium configuration:

$$\frac{\Delta h(t)}{h_0} = \frac{F}{2\pi R^2 G}\left[1 - \exp\left(\frac{-8Gk}{\eta R^2}t\right)\right], \quad (1)$$

where $\Delta h(t)=h(t) - h_0$ is the incremental change of film thickness, h_0 is the initial film thickness, F is the applied force, which is negative when the sample is compressed, G is the shear modulus, and t is the time. As follows from Eq. (1), the limiting deformation as $t \to \infty$ is written as

$$\Delta h / h_0 = \frac{F}{2\pi R^2 G}. \quad (2)$$

Thus, analyzing the limiting deformation, we can extract the shear modulus of the material G. Having given this modulus G, we can estimate the sample permeability by fitting the experimental data by the exponential curve (1). Therefore, these formulas (1)-(2) suggest a straightforward way to measure the in-plane permeability of the samples by monitoring the change of the film thickness as a function of time. Moreover, formulas (1)-(2) provide the basis for engineering design of the probing means using the nanofibrous materials. The measured permeability and shear modulus of the probing material can be further used to predict the dosing kinetics and the amount of liquid available for testing, provided that the applied load F is fixed.

CHARACTERIZATION DEVICE

The characterization device is shown in *Fig. 3a*. The plates and the sample, which is sandwiched between them, are placed on the reference stand. The load attached to a rod-connector, pulls the arm down, thus forcing the cross-plate to press the sample. A cross-plate transferring the load to the sample is attached to a movable beam. This beam is connected to a Linear Voltage Differential Transformer (LVDT), (Schaevitz MHR 025). LVDT measures and records the changes of the sample thickness. The thickness change of the sample is then transferred to a PC.

As follows from equation (1), the incremental change of the sample thickness depends only on the elastic properties of the sample and on its permeability. The density and porosity do not contribute to the sample reaction at the late stage of viscoelastic relaxation. Therefore, to eliminate the inertial contribution, one has to experimentally adjust the rate of the load release.

In our experiments, the application of different weights sometimes led to a non-reproducible stress-strain behavior at $t \rightarrow \infty$. In other words, the transition from elastic to hydraulic reaction was difficult to separate. We, therefore, modified the approach. Instead of placing different weights directly on the disc attached to the rod-connector, we preloaded the sample using the spring-on-threaded-rod system to balance a preload, (*Fig 3b*). This allowed us to apply the constant load gently, with a full confidence that the force is constant and the LVDT reading is not affected by a complex wave-like elastic reaction from the sample.

To check the reliability of this design, we made five measurements of the arm deflection without any sample. The arm deflection due to application of 100 gram load was measured by LVDT. We obtained 1.52 μm average deflection. As expected, we observed almost twice greater displacement when the load as twice increased, namely, 3.05μm average displacement at 200g.

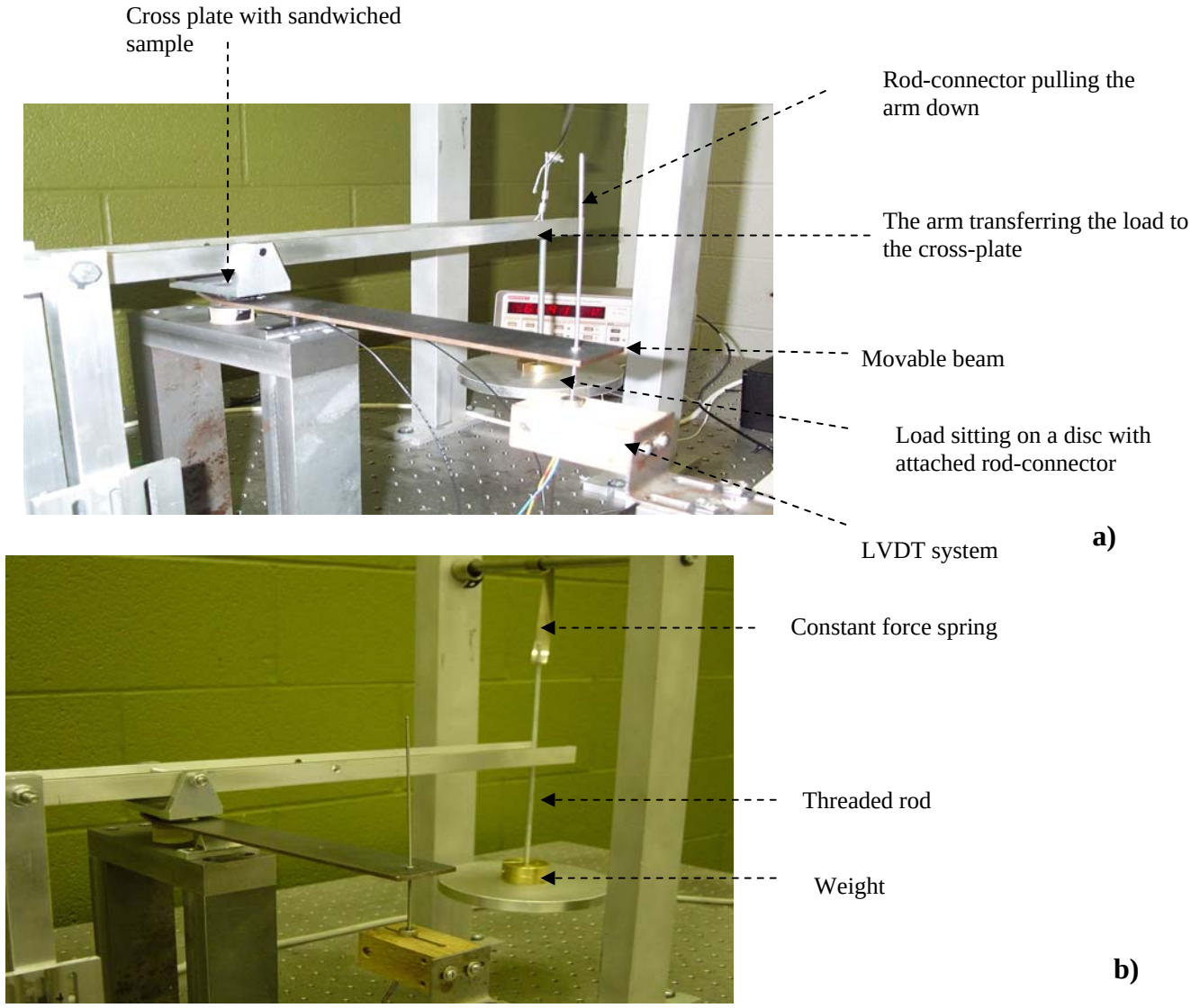

FIGURE 3. The characterization device. a) Layout of the measuring system equipped with LVDT and loading means, b) Layout of the load application system equipped with the spring. The sample is preloaded by the weight and the loading frame is supported by a constant force spring.

EXPERIMENTS

The nanowebs with and without mineral oil with the viscosity of η=27 cP, and the oil density of ρ= 0.914 g/cm^3 were tested by loading and unloading the samples. The sample porosity was estimated by saturating the samples with the mineral oil and then weighting the samples. From these experiments we estimated the porosity as m ~ 0.85-0.9. These values are comparable with typical porosity of napkins and other absorption articles [23]

As shown in *Fig.4a)*, the samples without oil demonstrate a visible hysterisis which can be attributed to some plastic deformations of the nanofibers. These deformations are manifested through appearance of some flat and distorted nanofibers in SEM micrograph, *Fig.4b)*. Within the same range of loads, the deformations of oil-saturated samples follow reversible pathway which is almost linear in the stress-strain graph *(Fig.4a)*. The data points were taken when the sample deformations had approached the limiting plateaus shown in *Fig.5a) and 5b)*.

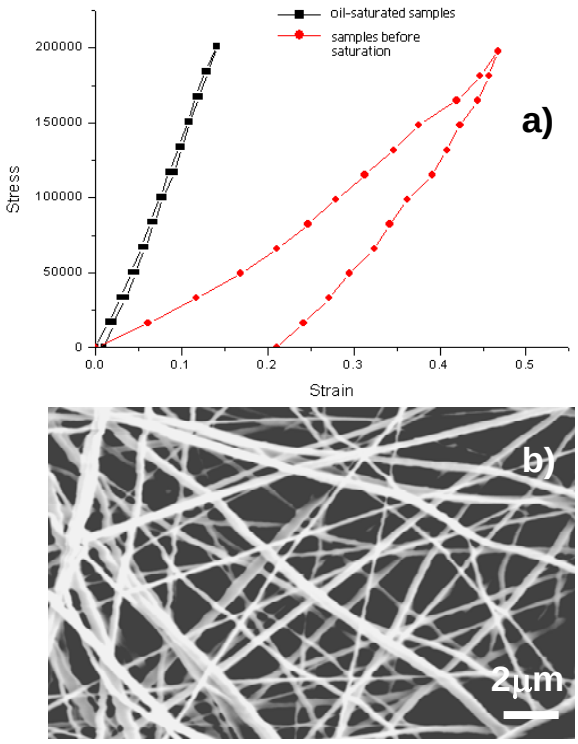

FIGURE 4. a) Hysteresis of sample deformations without oil. In the oil-saturated samples the deformations are reversible. The strain is the ratio of the incremental change of the thickness to initial thickness of the sample. b) Dry nanoweb after compression.

It is interesting to observe that the load supported by the flowing liquid inside the samples is sufficiently large. Even for the loads corresponding to plastic irreversible deformations of dry samples, the oil-saturated samples still deform reversibly with compression modulus defined as E =2G ~ 1.42 MPa and estimated from Eq. (2).

We experimented with the webs of thickness h_0 ~ 200μm and area πR^2 ~ 2.4 cm^2. The 1%-10% deformations ($\Delta h / h_0$ = 1%-10%) of these samples correspond to the oil release in the range $V = \pi R^2 \Delta h \sim$ 5·10^{-4}-5·10^{-3}cm^3. This microliter amount of liquid is probably collected at the edges of the samples. When the weight is released, the liquid comes back to fill the empty pores.

TRANSPORT PROPERTIES

We studied the relaxation phenomenon on the samples cut from the same piece of electrospun nanoweb. The samples were preloaded with different initial weights then the loads were increased with 100g increments. All samples showed the similar behavior, *Fig. 5 a,b). Fig 6 a,b*) show two typical reactions of the nanowebs. Sometimes we observed the sample relaxation with one characteristic relaxation time, as shown in *Fig. 6a)*. Sometimes another, shorter relaxation time, showed up, as seen from *Fig. 6b)*. In these graphs, as the load increases, the relaxation time decreases. This observation suggests that the nanowebs should have some other deformation mechanism which is not captured by our model. For example, a linear dry friction between fibers might contribute to this relaxation process.

As predicted by equation (1), the curves are expected to follow the exponential behavior, $\Delta h/h_0 = b$ (1-exp(-t/τ)) with one characteristic relaxation time τ, and constants b and τ defined in equation (1). From *Fig. 6a*, we found the average relaxation time as τ = 128.41 s. Using the definition of the relaxation time as given by (1), $\tau = \eta R^2 / (8Gk)$, and taking the measured shear modulus G = 0.71 MPa, the oil viscosity, η = 0.27 Pa·s, and the samples size R ~ 0.87cm, we found the permeability k = 2.8.10^{-14} m^2.

To check if the obtained number is reasonable, we compared this permeability value with the value obtained from the Kozeny-Carman equation [24]. For randomly packed fibrous materials the Kozeny-Carman equation is written in the form $k=m^3/(4a(1-m)^2)\, r^2$, where r is the fiber radius, and a ~ 5.3 is the

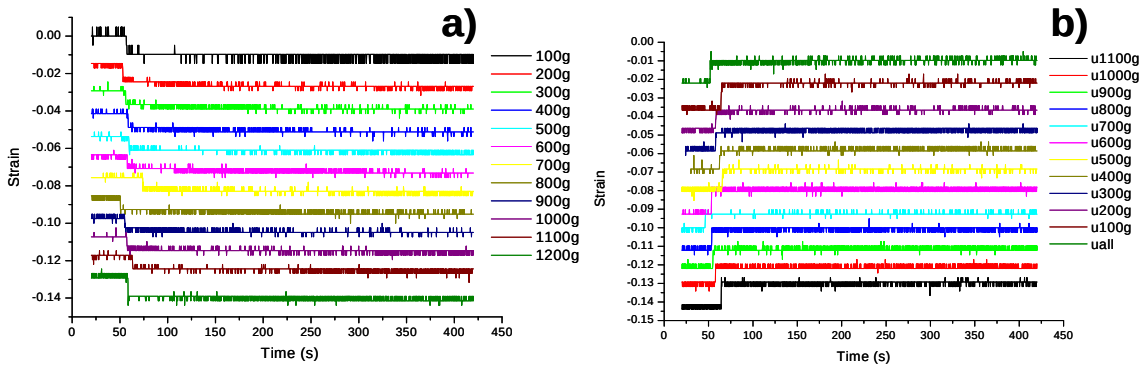

FIGURE 5. Strain relaxation upon loading (a) and unloading (b) of the oil-saturated samples.

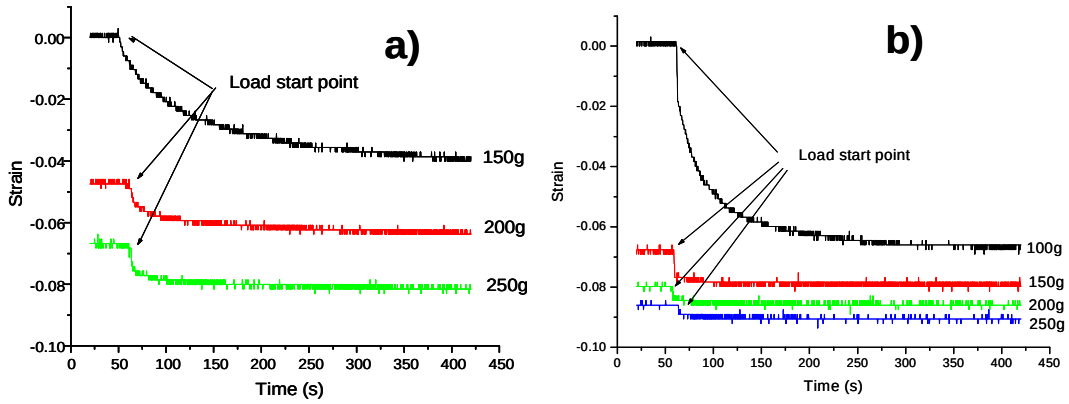

FIGURE. 6. Strain relaxation in two different samples a) sample subjected to 150g initial load with 50g step-wise increasing load; b) sample subjected to 100g initial load with 50g step-wise increasing load.

Kozeny-Carman constant which was found experimentally in Ref. [24]. Substituting the value $k = 2.8.10^{-14}$ m^2 and using the average porosity for our samples m =0.87, we obtain r ~ 124 nm. An inspection of the SEM micrographs shown in *Figs. 1, 4b)* confirms that this estimate of the nanofiber radius is reasonable. Thus, the proposed experimental method provides reliable results.

DISCUSSION AND CONCLUSION

We propose an idea to use electrospun nanowebs as probing and dosing materials. Due to nanopores formed by nanofiber crossings, the nanofibrous webs exert extremely high capillary pressure. This results in an enhanced absorption action as compared to existing fibrous absorbers. We found that typical porosity of electrospun nanowebs varies between 85-90 percents. Therefore, the absorption capacity of these materials is sufficient for probing purposes.

In many applications dealing with minute amount of liquids, electrospun nanowebs are proven to be very useful as dosing materials. Our experiments confirmed that the deformations of the oil-saturated nanowebs produced from P(VDF-TrFE) do not exceed 12%. This implies that extremely small liquid doze could be squeezed from the samples.

We found that if the stresses are less than 200KPa, the oil-saturated nanowebs behave as linear elastic bodies. The relaxation to equilibrium state follows the Voigt model of viscoelasticity. While in the Voigt model the relaxation time is a phenomenological parameter, the relaxation time of our samples depends on the elastic and transport properties of the nanowebs. We showed that if the applied loads are less than 200KPa one can safely assume that the

fibers in liquid-saturated nanowebs are incompressible. At the same time, the pore size in the sample changes because of the nanofiber bending, and, probably reversible sliding of one fiber over the other. This leads to a reversible process of sample deformation. Based on these arguments, we derived equations (1) and (2) which explain the Voigt-type relaxation process in the liquid-saturated nanowebs.

These equations suggest a straightforward way to simultaneously measure the in-plane permeability of nanofibrous materials and the materials elasticity. We showed that the in-plane permeability and shear modulus can be obtained by using the dynamic method of loading of the sample sandwiched between two impermeable plates. This dynamic method takes a few minutes to characterize the in-plane permeability and elasticity of soft nanoporous materials.

APPENDIX

Consider a thin porous layer fully saturated with some liquid and subjected to compression in the direction perpendicular to the sample plane. The balance of stresses in the sample is described by the following equation [10]

$$\nabla_k \left[(1-m)\sigma_{ki} - mp\delta_{ki} \right] = 0, \; i,k = 1,2,3, \quad \text{(A1)}$$

where m is the sample porosity, i.e. the volume of voids divided by the volume of the whole sample, σ_{ik} is elastic stress, $\delta_{i,k}$ is the Kronecker delta, and p is the pressure in the liquid.

Assuming that the liquid and solid phases are incompressible, i.e. their densities are constants, the mass balance written for the liquid and solid skeleton gives the following equations:

$$\frac{\partial m}{\partial t} + \nabla \cdot m\mathbf{V} = 0, \quad \text{(A2)}$$

$$\frac{\partial (1-m)}{\partial t} + \nabla \cdot (1-m)\mathbf{U} = 0. \quad \text{(A3)}$$

where ***V*** is the fluid velocity and ***U*** is the velocity of solid particles in the sample. Summing up both equations (A2) and (A3), we obtain the equation:

$$\frac{\partial \theta}{\partial t} + \nabla \cdot \mathbf{q} = 0. \quad \text{(A4)}$$

where $\theta = \nabla \cdot \mathbf{u}$ is the dilatation, i.e. the change of the skeleton volume, **u** is the displacement vector, i.e. the displacement of the skeleton particle having currently the coordinate **R** relative to its initial position $\mathbf{R_0}$, $\mathbf{u = R - R_0}$, and **q** is the flux, $\mathbf{q} = m\mathbf{(V-U)}$, $\mathbf{U} = \partial \mathbf{u}/\partial t$. The flux is related to the pressure gradient through the Darcy's law,

$$\mathbf{q} = -\frac{k}{\eta}\nabla p, \quad \text{(A5)}$$

where k is the sample permeability. Substituting (A5) in (A4), the latter is rewritten in the form

$$\frac{\partial \theta}{\partial t} = \frac{1}{\eta}\nabla \cdot k\nabla p. \quad \text{(A6)}$$

Thus, the pressure field is coupled with the deformation field. Even for small deformations, when the permeability is almost constant, the pressure depends on the deformation field. In our model, because the samples do not expand in plane, we will consider only uniform compression of the sample, i.e. $\theta = \theta(t)$. In general case, the deformations of the sample are allowed to be large. Therefore, we will use the Hencky strain [25] to relate the strain with the displacement of the plates. Therewith,

$$\theta = \ln(h/h_0), \quad \text{(A7)}$$

where h_0 is the initial sample thickness. Substituting this equation into (A6), we find

$$\frac{dh}{hdt} = \frac{k(\theta)}{\eta}\Delta p, \quad \text{(A8)}$$

where Δ is the Laplace operator. Because the sample thickness is assumed small, h<<R, we can introduce an average pressure and consider this pressure as a characteristic physical parameter of flow, $(2/h)\int_0^{h/2} p dz = P(r,t)$. To find the equation for this average pressure, we integrate (A8) through the sample thickness:

$$\frac{dh}{hdt} = \frac{k(\theta)}{\eta}\left(\Delta_{\perp}P + \frac{2}{h}\frac{\partial p}{\partial z}\bigg|_{z=h/2}\right)$$
$$= \frac{k(\theta)}{\eta}\Delta_{\perp}P$$

or

$$\frac{dh}{hdt} = \frac{k(\theta)}{\eta r}\frac{d}{dr}\left(r\frac{dP}{dr}\right). \qquad \text{(A9)}$$

Integration of (A9) and accounting for the boundary conditions that the pressure at the sample axis must be finite and the pressure outside the sample is atmospheric (it is zero in our calibration), leads to the solution

$$P = \frac{\eta}{4k(\theta)h}\frac{dh}{dt}\left(r^2 - R^2\right). \qquad \text{(A10)}$$

The stress acting on the upper plate consists of the stress exerted by the fibrous skeleton and by the pressure. Therefore, the force balance gives

$$F = 2\pi R^2 G\ln\left(h/h_0\right) + \frac{\pi\eta R^4}{4kh}\frac{dh}{dt}. \qquad \text{(A11)}$$

where we used the Hooke's law to relate the Hencky's strain with the stress, $\sigma_{zz} = 2G\theta$, and $2G$ is the shear modulus of the fibrous sample made of incompressible fibers [10]. Approximating the permeability as $k = k_0 + K\ln h/h_0$, which is a good approximation for linear elasticity and thus a continuation of the same elastic law onto the range of large deformations, we will have

$$F = 2\pi R^2 G\ln\left(h/h_0\right) + \frac{\pi\eta R^4}{4\left(k_0 + K\ln(h/h_0)\right)h}\frac{dh}{dt} \qquad \text{(A12)}$$

For small deformations,

$$\ln(h/h_0) = \ln(1 + \Delta h/h_0) \approx \Delta h/h_0,$$

this relation is transformed to a familiar Voigt model for viscoelastic materials [1],

$$F = 2\pi R^2 G\Delta h/h_0 + \frac{\pi\eta R^4}{4k_0 h_0}\frac{d\Delta h}{dt}, \qquad \text{(A13)}$$

with a typical exponential relaxation upon loading by a constant force

$$\Delta h/h_0 = \frac{F}{2\pi R^2 G}\left[1 - \exp\left(\frac{-8R^2 G k_0}{\eta R^4}t\right)\right] \qquad \text{(A14)}$$

At initial instants of time, $t \to 0$ we can use asymptotic expansion of (A14) truncated at the second term:

$$\Delta h/h_0 = \frac{4Fk}{\pi R^4\eta}t. \qquad \text{(A15)}$$

In other words, at the first moments, the rate of deformation is constant and proportional to the applied force.

When the load is not small and the deformations are perceptible, integration of (A12) is also possible, but it leads to an unpleasant expression. It is easier to calculate this equation numerically for particular physical parameters. The limiting strain is found immediately from (A12) as

$$h^*/h_0 = \exp\left[F/2\pi R^2 G\right].$$

Relaxation to this strain is also exponential,

$$h = h^* + \Delta h,$$

$$\Delta h/h_0 = A\exp\left(\frac{-8R^2 G\left(k_0 + K\ln h^*/h_0\right)}{\eta R^4}t\right) \qquad \text{(A16)}$$

with the amplitude A which depends on a prehistory of loading. It is seen, that for large deformations, the relaxation time depends on the strain. Namely, instead of k_0 and m_0 we must use the permeability and porosity of the material deformed to the strain h^*/h_0.

ACKNOWLEDGEMENTS

We acknowledge discussions with I.Tyomkin on applicability of the LVDT to measure small deformations of the nanowebs. K.G.K. is supported by the NSF (grant CMMI 0826067) and the Department of Commerce through the National Textile Center (grant M08-CL10).

BIBLIOGRAPHY

[1] Larson, R. G., "The structure and rheology of complex fluids", (ed. Gubbins, K. E.) (Oxford University Press, New York, 1999).

[2] Reneker, D. H. & Yarin, A. L. "Electrospinning jets and polymer nanofibers", *Polymer* **49**, 2387-2425 (2008).

[3] Rutledge, G. C. & Fridrikh, S. V. "Formation of fibers by electrospinning", *Advanced Drug Delivery Reviews* **59**, 1384-1391 (2007).

[4] Dzenis, Y., "Materials science - Structural nanocomposites", *Science* **319**, 419-420 (2008).

[5] Filatov, Y., Budyka, A. & Kirichenko, V. "*Electrospinning of Micro- and Nanofibers: Fundamentals in Separation and Filtration Processes"* (Begell House Inc, Redding, CT 2007).

[6] Neimark, A. V. et al., "Hierarchical Pore Structure and Wetting Properties of Single Wall Carbon Nanotube Fibers", *Nano Letters* **3**, 419-423 (2003).

[7] Alimov, M. M. & Kornev, K. G. "Impregnation of liquids into a laminated porous material with a high permeability contrast", *Physics of Fluids* **19**, 102108 (2007).

[8] Kornev, K. G., Burstyn, H. & Kamath, Y., "Electroimpregnation of yarns and fabrics with nonwetting liquids", *Journal of Applied Physics* **101** (2007).

[9] Detournay, E. & A.H.D., C. in *Comprehensive Rock Engineering* (ed. Hudson, J.) 113-169. (Pergamon Press, 1994).

[10] Wang, H. F., "*Theory of Linear Poroelasticity with Applications to Geomechanics and Hydrogeology"* (Princeton University Press, Princeton, NJ, 2000).

[11] Abrate, S., " Resin flow in fiber preforms" *Appl Mech Rev* **55**, 579-599 (2002).

[12] Coussy, O. *Poromechanics* (John Wiley and Sons, Chischester, 2004).

[13] Sommer, J. L. & Mortensen, A., " Forced unidirectional infiltration of deformable porous media", *Journal of Fluid Mechanics* **311**, 193-217 (1996).

[14] Michaud, V. & Manson, J. A. E. "Impregnation of compressible fiber mats with a thermoplastic resin. Part I: Theory", *Journal of Composite Materials* **35**, 1150-1173 (2001).

[15] Scherer, G. W. "Measuring permeability of rigid materials by a beam-bending method: I, theory", *Journal of the American Ceramic Society* **83**, 2231-2239 (2000).

[16] Scherer, G. W. "Measuring permeability of rigid materials by a beam-bending method: III, Cement paste", (vol 85, pg 1537, 2002). *Journal of the American Ceramic Society* **87**, 1615-1615 (2004).

[17] Lukas, D., Sarkar, A. & Pokorny, P. "Self-organization of jets in electrospinning from free liquid surface: A generalized approach", *Journal of Applied Physics* **103**, 084309 (2008).

[18] Reneker, D. H. & Chun, I. "Nanometre diameter fibres of polymer, produced by electrospinning", *Nanotechnology* **7**, 216-223 (1996).

[19] Dzenis, Y., "Spinning continuous fibers for nanotechnology", *Science* **304**, 1917-1919 (2004).

[20] Ren, X., "Nanomanufacturing and Analysis of Novel Continuous Ferroelectric PVDF and P(VDF-TrFE) Nanofibers", PhD Thesis, University of Nebraska-Lincoln , Lincoln, NE (2006) .

[21] Beil, N. B. & Roberts, W. W. "Modeling and computer simulation of the compressional behavior of fiber assemblies - I: Comparison to van Wyk's theory", *Textile Research Journal* **72**, 341-351 (2002).

[22] Carnaby, G. A. & Pan, N. "Theory of the Compression Hysteresis of Fibrous Assemblies", *Textile Research Journal* **59**, 275-284 (1989).

[23] Chatterjee, P. K. & Gupta, B. S. (eds.) *Absorbent Technology* (Elsevier, New York, 2002).

[24] Rahli, O., Tadrist, L., Miscevic, M. & Santini, R. "Fluid flow through randomly packed monodisperse fibers: The Kozeny-Carman parameter analysis", *Journal of Fluids Engineering-Transactions of the Asme* **119**, 188-192 (1997).

[25] Hencky, H. "The law of elasticity for isotropic and quasi-isotropic substances by finite deformations", *Journal of Rheology* **2**, 169-176 (1931).

AUTHORS' ADDRESSES

Kostantin G. Kornev
School of Materials Science & Engineering
Clemson University
264 Sirrine Hall
Clemson, SC 29634-0971
UNITED STATES

Xi Ren, Yuris Dzenis
Department of Engineering Mechanics
University of Nebraska-Lincoln
W317.4 Nebraska Hall
P.O. Box 880526
Lincoln, NE 68588
UNITED STATES